The Astrophysical Journal, 686:219–229, 2008 October 10

THE BLAST WAVE MODEL FOR AGN FEEDBACK: EFFECTS ON AGN OBSCURATION

N. Menci,[1] F. Fiore,[1] S. Puccetti,[1,2] and A. Cavaliere[3]

Received 2008 February 28; accepted 2008 June 26

ABSTRACT

We compute the effect of galactic absorption on active galactic nucleus (AGN) emission in a cosmological context by including a physical model for AGN feeding and feedback in a semianalytic model of galaxy formation. This is based on galaxy interactions as triggers for AGN accretion and on expanding blast waves as a mechanism to propagate outwards the AGN energy injected into the interstellar medium at the center of galaxies. We first test our model against the observed number density of AGNs with different *intrinsic* luminosities as a function of redshift. The model yields a "downsizing" behavior in close agreement with the observed one for $z \lesssim 2$. At higher redshifts, the model predicts an overall abundance of AGNs (including Compton-thick sources) larger than the observed Compton-thin sources by a factor of ≈ 2 for $z \gtrsim 2$ and $L_X \leq 10^{44}$ erg s^{-1}. Thus, we expect that at such luminosities and redshifts, Compton-thick sources contribute to about 1/2 of the total AGN population. We then investigate the dependence of the absorbing column density N_H associated with cold galactic gas (and responsible for the Compton-thin component of the overall obscuration) on AGN luminosity and redshift. We find that the absorbed fraction of AGNs with $N_H \geq 10^{22}$ cm^{-2} decreases with luminosity for $z \leq 1$. In addition, the total (integrated over luminosity) absorbed fraction increases with redshift up to $z \approx 2$, and saturates to the value ≈ 0.8 at higher redshifts. Finally, we predict that the luminosity dependence of the absorbed fraction of AGNs with $L_X \leq 3 \times 10^{44}$ erg s^{-1} will weaken with increasing redshift. We compare our results with recent observations and discuss their implications in the context of cosmological models of galaxy formation.

Subject headings: galaxies: clusters: general — galaxies: evolution — galaxies: formation

1. INTRODUCTION

The accretion that built up the supermassive black holes (SMBHs) now hosted in many local galaxies is widely thought to be associated with a sequence of output episodes observed as active galactic nuclei (AGNs). Since only a minority ($\sim 10^{-2}$; see Richstone et al. 1998) of local galaxies host a currently active AGN, the corresponding lifetimes are estimated to be close to $\tau \sim 10^8$ yr. Several observations indicate that the accretion episodes are fundamentally related to galaxy growth; one such indication is provided by the narrow scatter in the observed correlation of the SMBH mass M_{BH}, with host galaxy mass M, when the former is in the range $10^7 \leq M_{BH}/M_\odot \leq 10^9$ (Ferrarese & Merritt 2000; Gebhardt et al. 2000). The emissions of AGNs thus may conceivably constitute a probe for the history of accretion and growth of SMBHs, and for its interplay with the galaxy-building process.

The coevolution of galaxies and AGNs and their so-called "downsizing" (faster evolution for more luminous objects) also depends on feedback between nuclear and other galactic activities. In fact, the density of high-luminosity QSOs peaks at high redshift and declines strongly afterward; similarly, massive galaxies are characterized by a star formation history that peaks at high redshifts. Luminous AGNs are efficient in "sterilizing" their massive host galaxies by heating the interstellar matter through winds, shocks, and high-energy radiation (e.g., Granato et al. 2004; Murray et al. 2005; Hopkins et al. 2006; Bower et al. 2006; Menci et al. 2006); intriguingly, these authors found that the bimodal color distribution of galaxies at $z \gtrsim 1.5$ can only be explained if AGN feedback is considered. In this picture, an AGN phase precedes the phase when a galaxy is caught in a passive state with red optical–UV colors, most of the star formation having been inhibited by AGN activity. Indeed, Pozzi et al. (2007) found using *Spitzer* photometry that a sample of optically obscured QSOs at $z = 1$–2 are mainly hosted by red passive galaxies, suggesting a later stage in their evolution.

On the other hand, many weak AGNs have been found at low redshift in star-forming galaxies (Salim et al. 2007). In these cases, feedback from less powerful AGNs (the so-called "radio mode") is probably acting to self-regulate accretion and star formation, and cold gas is left available for both processes for a much longer time (Croton et al. 2006). The same cold gas can intercept the line of sight to the nucleus. Indeed, Compton-thin absorbers (with column densities $N_H \leq 10^{24}$ cm^{-2}) may well be located in the galactic disk (Malkan et al. 1998; Matt 2000; see also Ballantyne et al. 2006). Therefore, a natural expectation in this scenario is that the fraction of obscured AGNs will be large at low AGN luminosities. It is well known since the pioneering work done with the *Einstein* satellite (Lawrence & Elvis 1982) and with optically and radio-selected AGNs (Lawrence 1991) that this fraction strongly decreases with increasing AGN luminosity (see Ueda et al. 2003; La Franca et al. 2005; Gilli et al. 2007; Triester et al. 2008; Hasinger 2008). A widely shared view holds that the luminosity dependence of the obscured fraction is related to the energy fed back by the AGNs into the surrounding gas that constitutes the interstellar medium (ISM). Given that the AGN emission is proportional to the fraction of such a gas available for accretion, a *positive* correlation between luminosity and absorption would be expected in the absence of energy feedback that depletes the ISM at the onset of AGN activity.

A mounting body of observations cogently indicates that strong nuclear feedback is present in galaxies hosting AGNs (for a review, see Elvis 2006 and references therein). On small (subparsec)

[1] INAF-Osservatorio Astronomico di Roma, via di Frascati 33, I-00040 Monteporzio, Italy.
[2] ASI SDC, % ESRIN via Galileo Galilei, I-00044 Frascati, Italy.
[3] Dipartimento di Fisica, Università di Roma Tor Vergata, via Ricerca Scientifica 1, I-00133 Roma, Italy.

scales, the observed X-ray absorption lines indicate the presence of outward winds with velocities up to some 10^4 km s^{-1} (Weymann 1981; Turnshek et al. 1988; Crenshaw et al. 2003; Chartas et al. 2002; Pounds et al. 2003; Pounds & Page 2006; Risaliti et al. 2005a). These likely originate from the acceleration of disk outflows due to the AGN radiation field (Proga 2007 and references therein). On larger scales, broad absorption lines in about 10% of optically luminous QSOs indicate fast outflows (up to 30,000 km s^{-1}). Massive (10–50 $M_\odot$ yr^{-1}) flows of neutral gas with speeds of $\sim$1000 km s^{-1} are observed through 21 cm absorption of radio-loud AGNs (see Morganti et al. 2005), indicating that AGNs have a major effect on the circumnuclear gas in the central kiloparsec region around AGNs. On even larger scales of some 10^2 kpc, the presence of AGN-induced outflows is revealed by X-ray observations of the intracluster medium (see McNamara & Nulsen 2007 for a review) showing cavities and expanding shocks with Mach numbers ranging from $\sim$1.5 to $\sim$8. How the outflows produced in the innermost regions of the active galaxies are transported outwards to affect such large scales is still a matter of investigation. Buoyant bubbles (see Reynolds et al. 2001; Churazov et al. 2001) and expanding blast waves (see Cavaliere et al. 2002; Lapi et al. 2005) constitute viable mechanisms for such a transport.

Nuclear obscuration is directly linked to AGN feedback, since the same gas (and dust) that feeds the AGN energy output may well be responsible for its obscuration. Therefore, modeling AGN obscuration is essential to connect the observed AGN properties to the accretion history of SMBHs over cosmological time. This is a significant theoretical challenge, as it requires not only connecting AGN evolution to galaxy formation and growth, but also implementing in a model a self-consistent description of AGN feedback into galactic gas. Indeed, very few attempts have been carried out in this direction so far. An attempt to include AGN absorption into an ab initio galaxy formation model was proposed by Nulsen & Fabian (2000) by relating both the SMBH fueling and the AGN absorption to the cooling flows associated with the hot gas that pervades the growing dark matter halos, but this assumption did not lead to a full description of the statistical distribution of QSO luminosity.

Here, we develop our semianalytic model of hierarchical galaxy formation and AGN evolution (see Menci et al. 2006) to self-consistently include the absorption of AGNs, with the aim of investigating cosmic AGN evolution and its dependence on AGN properties such as luminosity and redshift. The model is suited to our scope, as it includes a close treatment of the feedback into the interstellar gas. Our aim is to investigate the dependence of AGN absorption on luminosity L and redshift z arising in hierarchical galaxy formation scenarios that include an effective description of the evolution of AGNs and of their feedback.

The plan of the paper is as follows. In § 2, we describe our model for galaxy formation and the associated AGN evolution. Section 3 is focused on describing our treatment of AGN feedback into the interstellar gas and its effects on AGN absorption. In § 4, we test our feedback-inclusive model for AGN evolution by comparing its outcome with the redshift distribution of the number density of AGNs for different X-ray luminosities. Our results on the luminosity and redshift dependence of the absorbed fraction of AGNs are shown and discussed in § 5, and a summary of our conclusions is given.

2. THE MODEL

The semianalytic model we develop and use connects, within a cosmological framework, accretion onto SMBHs and the ensuing AGN activities with the evolution of galaxies.

2.1. *Hierarchical Galaxy Evolution*

Galaxy formation and evolution are driven by the collapse and growth of dark matter (DM) halos, which originate by the gravitational instability of overdense regions in the primordial DM density field. This is taken to be a random, Gaussian density field with a cold dark matter (CDM) power spectrum within the "concordance cosmology" (Spergel et al. 2007), for which we adopt round parameters $\Omega_\Lambda = 0.7$, $\Omega_0 = 0.3$, baryonic density $\Omega_b = 0.04$, and Hubble constant (in units of 100 km s^{-1} Mpc^{-1}) $h = 0.7$. The normalization of the spectrum is taken to be $\sigma_8 = 0.9$ in terms of the variance of the field smoothed over regions of 8 h^{-1} Mpc.

As cosmic time increases, larger and larger regions of the density field collapse, and eventually lead to the formation of groups and clusters of galaxies; previously formed, galaxy-sized condensations are enclosed. The process implies not only smooth mass inflow, but also merging and coalescence of smaller condensations. The corresponding merging rates of the DM halos are provided by the extended Press & Schechter formalism (see Bond et al. 1991; Lacey & Cole 1993). The clumps included in larger DM halos may survive as satellites, merge to form larger galaxies through binary aggregations, or coalesce into the central dominant galaxy due to dynamical friction. These processes take place over timescales that grow longer over cosmic time, so the number of satellite galaxies increases as the DM host halos grow from groups to clusters. All the above processes are implemented in our model as described in detail in Menci et al. (2005, 2006), and based on canonical prescriptions of semianalytic modeling.

Radiative gas cooling, the ensuing star formation, and the supernova events with associated feedback that occurs in the growing DM halos (with mass m and circular velocity v) are described in our previous papers (e.g., Menci et al. 2005). The cooled gas with mass m_c settles into a rotationally supported disk with radius r_d (typically ranging from 1 to 5 kpc), rotation velocity v_d, and dynamical time $t_d = r_d/v_d$. The gas gradually condenses into stars at a rate $\dot{m}_* \propto m_c/t_d$; the ensuing stellar feedback returns part of the cooled gas to the hot gas phase with mass m_h at the virial temperature of the halo. An additional channel for star formation implemented in the model is provided by interaction-driven starbursts triggered not only by merging but also by fly-by events between galaxies. Such a star formation mode provides an important contribution to the early formation of stars in massive galaxies, as described in detail in Menci et al. (2004, 2005).

2.2. *Accretion onto SMBHs and AGN Emission*

The model also includes a treatment of SMBHs growing at the center of galaxies by interaction-triggered inflow of cold gas, following the physical model proposed by Cavaliere & Vittorini (2000) and implemented in Menci et al. (2006). The accretion of cold gas is triggered by galaxy encounters (both fly-by and merging encounters), which destabilize part of the cold gas available by inducing loss of angular momentum. In fact, small-scale (0.1–a few kpc) regions are likely to have disk geometry if they are to efficiently remove angular momentum and convey to (unresolved) parsec scales the gas provided on larger scales (these may be isotropized by head-on, major merging events).

The rate of such interactions is given by Menci et al. (2003) in the form

$$\tau_r^{-1} = n_T \Sigma(r_t, v, V_{\rm rel}) V_{\rm rel}. \quad (1)$$

Here, n_T is the number density of galaxies in the same halo, and $V_{\rm rel}$ is their relative velocity. Encounters effective for angular

momentum transfer require (1) the interaction time to be comparable with the internal dynamical times of the partner galaxies (a resonance condition), and (2) the orbital specific energy of the partners not to exceed the sum of their specific internal gravitational energies. The cross section Σ for such encounters is given by Saslaw (1985) in terms of the tidal radius r_t associated with a galaxy with given circular velocity v (see Menci et al. 2003, 2004).

The fraction of cold gas accreted by the BH in an interaction event is computed in terms of the variation Δj of the specific angular momentum $j \approx Gm/v_d$ of the gas (Menci et al. 2003):

$$f_{\rm acc} \approx 10^{-1} \left| \frac{\Delta j}{j} \right| = 10^{-1} \left\langle \frac{m'}{m} \frac{r_d}{b} \frac{v_d}{V_{\rm rel}} \right\rangle. \quad (2)$$

Here, b is the impact parameter, evaluated as the average distance of the galaxies in the halo. Also, m' is the mass of the partner galaxy in the interaction, and the average runs over the probability of finding such a galaxy in the same halo where the galaxy with mass m is located. The values of the quantities involved in the average are computed from the semianalytic model recalled in § 2.1, and yield values of $f_{\rm acc} \lesssim 10^{-2}$. For minor merging events and for encounters among galaxies with very unequal mass ratios $m' \ll m$, which dominate the statistics in all hierarchical models of galaxy formation, the accreted fraction takes values $10^{-3} \lesssim f_{\rm acc} \lesssim 10^{-2}$.

The average amount of cold gas accreted during an accretion episode is thus $\Delta m_{\rm acc} = f_{\rm acc} m_c$, and the duration of an accretion episode, i.e., the timescale for the QSO or AGN to shine, is assumed to be the crossing time $\tau = r_d/v_d$ for the destabilized cold gas component.

The time-averaged bolometric luminosity so produced by a QSO hosted in a given galaxy is then provided by

$$L = \frac{\eta c^2 \Delta m_{\rm acc}}{\tau}. \quad (3)$$

We adopt an energy conversion efficiency $\eta = 0.1$ (see Yu & Tremaine 2002), and derive the X-ray luminosities $L_{\rm X}$ in the 2–10 keV band from the bolometric corrections given in Marconi et al. (2004). The SMBH mass $m_{\rm BH}$ grows mainly through accretion episodes as described above, as well as through coalescence with other SMBHs during galaxy merging. As an initial condition, we assume small seed BHs of mass $10^2\ M_\odot$ (Madau & Rees 2001) to be initially present in all galaxy progenitors; our results are insensitive to the specific value, as long as it is smaller than some $10^5\ M_\odot$.

In our Monte Carlo model, at each time step we assign to a galaxy the interaction probability corresponding to the rate given in equation (1). According to that equation, we assign to the galaxy an active SMBH accretion event of duration τ. Then we compute the accreted cold gas and the associated AGN emission through equations (2) and (3).

3. AGN FEEDBACK AND COLUMN DENSITY OF ABSORBING GAS

The model for AGN evolution presented here, in contrast to the previous implementation by Menci et al. (2003, 2004), is complemented with the feedback from AGNs onto the surrounding ISM. This affects (1) the available cold gas left over in the galactic disk after each AGN event, which determines the subsequent gas accretion history, and (2) the density distribution of the galactic gas during each AGN event, which determines the AGN absorption.

3.1. *Blast Wave Model for AGN Feedback*

As mentioned in the introduction, fast winds with velocities up to $10^{-1}c$ are observed in the central regions of AGNs. They likely originate from the acceleration of disk outflows by the AGN radiation field (see Begelman 2003 for a review) and affect the environment in the host galaxy and beyond, leaving imprints out to large scales of some 10^2 kpc in the intracluster medium (ICM).

A detailed model for the transport of energy from the inner, outflow region to the larger scales has been developed by Cavaliere et al. (2002) and Lapi et al. (2005). Central, highly supersonic outflows compress the gas into a blast wave terminated by a leading shock front, which moves outwards with a lower but still supersonic speed and sweeps out the surrounding medium. Eventually, this is expelled from the galaxy; in the case of powerful shocks, it is expelled even from a group or poor cluster hosting the galaxy.

The key quantity determining all shock properties is the total energy ΔE injected by AGNs into the surrounding gas. This is computed as

$$\Delta E = \epsilon_{\rm AGN} \eta c^2 \Delta m_{\rm acc} \quad (4)$$

(see § 2.2) for each SMBH accretion episode in our Monte Carlo simulation; the value of the energy feedback efficiency for coupling with the surrounding gas is taken as $\epsilon_{\rm AGN} = 5 \times 10^{-2}$, which is consistent with the values required to match the X-ray properties of the ICM in clusters of galaxies (see Cavaliere et al. 2002). This is also consistent with the observations of wind speeds up to $v_w \approx 0.1c$ in the central regions, which yield $\epsilon_{\rm AGN} \approx v_w/2c \approx 0.05$ by momentum conservation between photons and particles (see Chartas et al. 2002; Pounds et al. 2003); this value has also been adopted in a number of simulations (e.g., Di Matteo et al. 2005) and semianalytic models of galaxy formation (e.g., Menci et al. 2006).

The blast expands into the ISM or the ICM as described by hydrodynamical equations that include the effects not only of initial density gradient, but also those of upstream pressure and DM gravity, clearly important quantities in galaxies, as discussed by Lapi et al. (2005). The solutions show in detail how the perturbed gas is confined to an expanding shell bounded by an outer shock at radius $R_s(t)$, which sweeps out the gas surrounding the AGN. The overall effects have been emulated in simulations by Di Matteo et al. (2005), as performed for specific cases of major mergers. Our treatment also covers the less energetic but more frequent events, with accretion rates and AGN energy inputs ΔE provided by equations (1)–(4). On the other hand, our model assumes spherical symmetry. Note, however, that this approximately holds in the central regions (the ones mainly affecting our results, as we shall show below) due to the exponential decline of the gas density. In addition, both of the effects discussed in points (1) and (2) of the Appendix (see § 3.2 below) make the average absorption even less dependent on the disk outside the central region. As for the outflow geometry, our model also applies to segments of spherical shells expanding outwards, generated by winds driven by a spherically symmetric AGN radiation field; these segments may not uniformly cover the central source, as in the conical distribution of Elvis (2000). While it is true that random lines of sight may not intercept some of these segments, the random orientation of the internal BH accretion disk with respect to the outer, galactic disk (Gallimore et al. 1997; Nagar & Wilson 1999; Thean et al. 2001) makes our results realistic on average. Finally, we do not consider clumpy outflows; however, these are not expected to affect the dependence of the column density distribution on AGN

luminosity and redshift, although they could broaden the column density distributions that we derive from our model.

Lapi et al. (2005) showed in detail how the hydrodynamical equations for the finite-amplitude gas perturbation constituting the blast wave, supplemented with the Rankine-Hugoniot boundary conditions at the shock, still admit self-similar solutions (see Sedov 1959) when gravity, initial gradients, and pressure are included. These solutions at a distance r from the center are expressed in terms of r/R_s, where $R_s(t)$ is the shock position after a time t from an AGN outburst; this is given by equation (C7) in Lapi et al. (2005), which we recast in the form

$$R_s(t) = v_d t_d \left[\frac{5\pi\omega^2}{24\pi(\omega-1)}\right]^{1/\omega} \mathcal{M}^{2/\omega} \left(\frac{t}{t_d}\right)^{2/\omega}, \qquad (5)$$

where $\mathcal{M}$ is the Mach number $\mathcal{M} = v/c_s[R_s(t)]$.

Here, the initial gas density has a radial profile given by a power law $\rho \propto r^{\omega}$, where the exponent is in the realistic range $2 \leq \omega < 2.5$. Although self-similar, analytical solutions for the shock expansion law can only be found for spherical (or, in general, one-dimensional) symmetry and power-law gradients, we shall also apply equation (5) to blasts expanding in the inner regions of a galactic disk, where the actual density profile follows an exponential law $\rho = (1/2h)\sigma_0 \exp(-r/r_d)$, where h is the disk thickness and σ_0 is the central surface density, with a cutoff in the vertical direction corresponding to the thickness of the disk. To use the above self-similar blast, we construct piecewise power-law approximations of the above exponential density by subdividing the radial disk coordinate into a sequence of shells; within each shell, the exponential decline is approximated by a power law with a different exponent ω. The expansion of the blast in each shell will be computed upon using equation (5) with the appropriate value of ω.

Self-similarity implies a definite time behavior for the AGN energy injection, which is determined by the exponent ω defining the density decline, normalized to reach its total value ΔE at the end of the accretion episode. In turn, this implies a well-defined form for the time decay of the AGN luminosity, as shown in the Appendix. However, in the self-similar solutions, the ratio $\Delta E/E$ between the energy injected up to a time t and the energy of the ISM within the shock radius $R_s(t)$ is shown to be independent of time and position (see Appendix); it thus constitutes the basic quantity determining the strength of the shock. In fact, the Mach number is shown to be simply related to $\Delta E/E$, which we compute at the final time of the AGN active phase. In the following, we shall take $\mathcal{M}^2 = 1 + \Delta E/E$, as derived by Lapi et al. (2005).

In terms of the rescaled variable r/R_s, the previous authors derived the density distribution; this is found to be confined to a shell close to R_s between the outer shock and an inner "piston" at a position $\lambda R_s(t)$ ($\lambda < 0.7$), with a width $(1-\lambda)R_s$, which is weakly dependent on the Mach number. Inside the shell, little gas is left over to absorb the AGN radiation.

3.2. *Effect of a Blast Wave on the Column Density of the Absorbing Galactic Gas*

The amount of unshocked gas absorbing the AGN emission will be given, for a given line of sight, by the time-dependent fraction still unperturbed outside the shock located at $r = R_s(t)$ (see Fig. 1). The faster the shock, the lower will be the fraction of still unperturbed gas outside $R_s(t)$ after a time t from an AGN outburst.

The dependence of $R_s(t)$ in equation (5) on the AGN luminosity will then affect the absorption by the unperturbed gas; in particular, for the case $\omega = 2$ (corresponding to the standard isothermal sphere), the relation $R_s(t) \propto \mathcal{M}t \propto (\Delta E/E)^{1/2}t$ holds, yielding a *lower* absorbing gas fraction outside $R_s(t)$ for *brighter* AGNs at a fixed time t.

An additional contribution to the absorption will be given by the gas compressed by the shock in a shell of width $(1-\lambda)R_s$ (see Lapi et al. 2005), where λ can be also expressed in terms of the relevant ratio $\Delta E/E$; however, we shall show that this second contribution depends only weakly on the AGN luminosity.

We implement the above model for AGN feedback and for absorption in our semianalytic model as follows.

1. For each galaxy in our Monte Carlo simulations, with disk exponential scale length r_d and total disk mass m_c computed as described in § 2.1, we assume for the density distribution of the unperturbed gas the simplified form $\rho = \rho_0 \exp(-r/r_d)$ (where r is the distance from the center of the galaxy), with a cutoff in the vertical direction (perpendicular to the disk) at $r = h$, corresponding to the disk thickness.

The value of the vertical scale height h for the *gaseous* disk is taken to be $r_d/15$ (see Narayan & Jog 2002), corresponding to ~200 pc for a typical L_* galaxy. With such a low value of h, our assumed density for the gaseous disk closely follows a constant vertical density distribution with a radial exponential profile $\exp(-x/r_d)$, where x is the distance from the center in the plane of the disk. The deviations are $\leq$14% in the central region and $\leq$1% at $x = r_d$. These are both smaller than the present uncertainty on the vertical distribution of the density of the gaseous disks; on the other hand, the above schematic form for the gas density distribution allows us to apply a simple analytical description for the evolution of the blast. The density distribution is normalized so as to recover the total gas mass m_c when integrated over the disk volume.

2. We construct a piecewise power-law approximation of the above exponential density distribution by subdividing the radial coordinate into shells. In each shell we approximate the exponential shape $\exp(-r/r_d)$ with a power law $Aq^{\omega}s^{-\omega}$, where $s = r + q$, and where q, A, and ω are parameters that we adjust to optimize the fit in each radial shell. We find that, on retaining $q = 1.8r_d$ at all radii, the following set of radial shells and parameters provides a good fit to the exponential law: $A = 1, \omega = 2$ for $r_m \leq r \leq r_d/2$; $A = 1.23, \omega = 2.3$ for $r_d/2 \leq r \leq 3r_d/2$; and $A = 1, \omega = 2.5$ for $r \geq 3r_d/2$. Here, the minimal radius considered is $r_m = 50$ pc. For the above choices, the rms deviation in the fits is $\Delta \leq 3\%$ within the inner region ($r \leq 10r_d$, the dominant range for the AGN absorption) and $\Delta \leq 30\%$ for $r \geq 10r_d$ (a region irrelevant to our computation of the AGN absorption). The temperature of the gas in the disk is assumed to be $T_d = 10^4$ K.

3. When a SMBH starts its accretion phase, triggered by a close interaction of the host galaxy with a companion, we compute the corresponding AGN total energy injection ΔE. For the sake of simplicity, we shall label each AGN with a constant luminosity L after equation (3), although full consistency with the self-similar solutions adopted for the blast wave expansion would require a time decay of the luminosity related to the exponent ω. However, we show in the Appendix that assuming a constant L yields results indistinguishable from those obtained by assigning exact, time-dependent luminosities to the AGNs.

4. During the time interval τ, we follow the expansion of the shock given by equation (5) for each radial shell defined in point (2), using the appropriate value of ω given by the fitting procedure described above. We compute the amount of gas still unperturbed outwards of the shock position $R_s(t)$ at a time t within the interval τ. The unshocked gas distribution is given

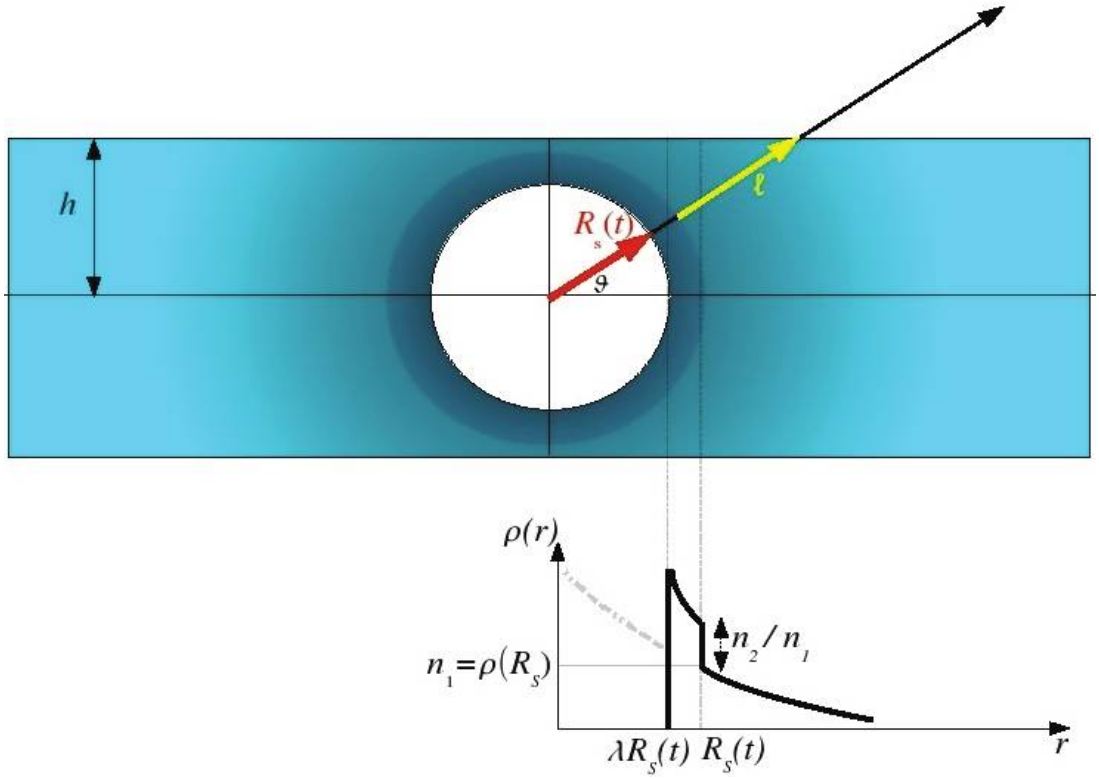

FIG. 1.—Schematic representation of the effect of the blast wave induced by AGN feedback on the density distribution of the interstellar gas. The shock radius $R_s(t)$ expands outwards, compressing the swept gas into a thin shell (*darker color*) with width $R_s(1-\lambda)$, and leaving a cavity inside. Such a density distribution $\rho(r)$ is also plotted at the bottom. A line of sight (at an angle θ with respect to the plane of the galactic disk) is also represented, along with the length ℓ of the line of sight intercepting the unperturbed gas in front of the shock.

by the density profile $\rho(r)$ defined in point (2), with $r \geq R_s(t)$ (see Fig. 1).

5. We extract a random line-of-sight angle θ, which defines the disk inclination to the observer. At a time t within the interval τ corresponding to the active AGN, we compute the column density corresponding to the gas outside the shock position along the selected line of sight as

$$N_{\rm H} = \int_{R_s(t)}^{h/\sin\theta} \rho(r)\, d\ell. \qquad (6)$$

6. If, for the chosen line of sight, the shock position is within the disk, we add the absorption column density corresponding to the gas compressed by the shock (see Fig. 1). Lapi et al. (2005) showed that the density of the gas swept by the blast and compressed to a shell of width $(1-\lambda)R_s$ rises toward the center as a function $D(r/R_s(t))$, which diverges weakly (but still integrates to a limited mass) at the piston position $\lambda R_s(t)$. On adopting the behavior $D(r/R_s(t)) = [(r/\lambda R_s) - 1]^{(\omega-6)/3(7-\omega)}$ (strictly valid on approaching the piston position), and integrating over r within the shocked shell, the corresponding column density is

$$N_{\rm H,shock} = \frac{15-5\omega}{3(7-2\omega)} \left(\frac{1}{\lambda} - 1\right)^{(15-5\omega)/[3(7-2\omega)]} \frac{n_2}{n_1} n_1 R_s(t). \qquad (7)$$

Here, n_2/n_1 is the density jump at the shock, and $n_1 = \rho(R_s)$ is the unperturbed gas density just outside the shock front. Both the density jump n_2/n_1 and λ grow slowly with increasing Mach number $\mathcal{M}$ (in turn, a function of $\Delta E/E$), as given in Lapi et al. (2005); both quantities saturate to constant values ($n_2/n_1 = 4$ and $\lambda \approx 0.7$) in the limit of very strong shocks ($\mathcal{M} \gg 1$).

In sum, the blast wave has two effects. On the one hand, it depletes the internal regions, thus decreasing the column density of the absorber (as computed in point [5] above). On the other hand, it increases the density inside a thin layer close to the piston (an effect computed in point [6] above). The first effect, however, dominates, since the gas initially distributed in the denser central region is spread out by the blast into an expanding spherical shell; thus, the integration along the line of sight intercepts only a tiny fraction of the gas initially concentrated in the core of the distribution. In addition, the minor contribution to the column density from equation (7) represents an upper limit, since the gas temperature in the blast wave is increased to values (given in eq. [C8] of Lapi et al. 2005) that generally exceed the ionization temperature of the gas, and thus limit the absorption. At the end of the AGN accretion episode (i.e., at $t = \tau$), only a fraction of the initial cold gas mass m_c will be left in the galaxy, as discussed in detail in Cavaliere et al. (2002) and Lapi et al. (2005). Note that the brighter the AGN is, the larger will be the injected energy ΔE, the faster will be the shock expansion $R_s(t)$ (see eq. [5]), and the lower will be the resulting column density at a given time after the start of the outburst (see eq. [6]).

Thus, the evolution of the gas distribution, and hence of the gas absorption, during the AGN event is best described in terms of the key ratio $\Delta E/E$, which determines all the relevant quantities of the blast: the expansion of the shock front $R_s(t)$, the thickness of the shocked shell $(1-\lambda)$, and the density jump at the shock. Such a ratio is computed in the model for each galaxy when an active accretion episode is triggered by a close encounter.

The effects of the above-detailed model for the AGN feedback on the evolution of cold galactic gas and on the galactic absorption of AGN emission are given below.

4. RESULTS

Here, we present our results concerning the evolution of the AGN number density and the obscuration by galactic interstellar gas. We do not provide a description of absorption due to the clouds within the central regions of AGNs, so we cannot disentangle Compton-thick sources (where the obscuration is presumably provided by gas in regions $r < 10$ pc) from the absorbed population we obtain from our model. Indeed, the shock may originate at any point within our resolution scale (50 pc), and it may lie inside or outside the Compton-thick region. Therefore, we cannot make any strong statement about the dependency of Compton-thick absorption on the outflow, and hence on the AGN luminosity.

Before addressing the problem of the luminosity and redshift dependence of AGN absorption, we test the basic predictions of our model with recent data. To this end, we first compare in Figure 2 the predicted evolution of the cosmic density of AGNs with different *intrinsic* luminosities L with data from La Franca et al. (2005). Note that the model reproduces the marked *downsizing* of AGNs, i.e., the faster redshift evolution of brighter AGNs compared to fainter sources (a behavior already obtained in semi-analytic models; see Menci et al. 2004; Fontanot et al. 2006). In the model, such an effect is related to the faster consumption of gas in the progenitors of massive galaxies at high redshifts $z \gtrsim 3$. In fact, these are formed in biased, high-density regions of the density field, where the early cooling of galactic gas provides early reservoirs for BH accretion, and the galaxy merging and interactions are enhanced. When such progenitors assemble to form a massive galaxy (and correspondingly a bright AGN when the BH is actively accreting) at $z \lesssim 2$, the available galactic gas has largely been converted into stars or accreted onto the BH at higher redshifts. Conversely, low-mass galaxies retain a large fraction of their gas down to low redshifts, and this results in prolonged star formation (yielding blue colors as observed) and allowance for effective BH accretion down to $z \approx 0$.

Note that at $z \gtrsim 2$, the model predictions lie above the observed points by a factor of $\approx$2 for low-luminosity AGNs with $L_X \leq 10^{43}$ erg s^{-1}. This, at least in part, is because the model predictions in Figure 2 concern all AGNs, regardless of whether they are Compton thin or Compton thick (since we cannot disentangle the two populations in our model), while the data we compare them with include only Compton-thin sources. A complementary check would be constituted by the X-ray background at its 30 keV peak (where observations are not affected by Compton-thick obscuration). However, this does not actually constitute a strong constraint from the model, since its main contributors are objects at $z \leq 2$ (Gilli et al. 2007), whose observed density is well reproduced by the model. We have repeatedly checked since Menci et al. (2003, 2004) that the basic features of our background model are consistent with the constraint set by the observed X-ray background (see Barcons et al. 2000), and that the predicted global history of BH assembly is consistent with the local observed SMBH mass function (Marconi et al. 2004).

Thus, the comparison between model predictions and observation strongly suggests the existence of a relevant fraction of Compton-thick sources at $z \gtrsim 1.5$ (as found by Martinez-Sansigre et al. 2005, 2007; Fiore et al. 2008a, 2008b). Note, however, that a complementary possibility, which could partly account for the model overestimate of low-luminosity sources at $z \gtrsim 2$, is that the BH growth in small-mass galaxy halos (DM masses $M \leq 10^9\ M_\odot$) is inhibited by a process not included in the model; we shall comment further on this point in our conclusions.

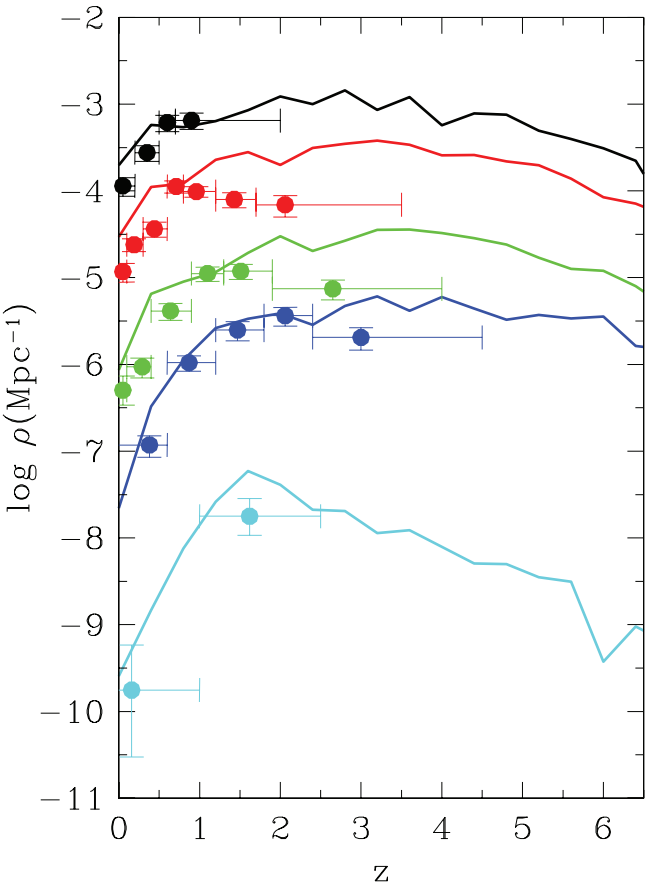

FIG. 2.—Evolution of the cosmic density of AGNs with X-ray luminosities (in the 2–10 keV band) in 5 different luminosity bins: $42 \leq \log L/\mathrm{erg\ s^{-1}} < 43$ (*black line*), $43 \leq \log L/\mathrm{erg\ s^{-1}} < 44$ (*red line*), $44 \leq \log L/\mathrm{erg\ s^{-1}} < 44.5$ (*green line*), $44.5 \leq \log L/\mathrm{erg\ s^{-1}} < 45$ (*blue line*), and $\log L/\mathrm{erg\ s^{-1}} \geq 45$ (*cyan line*). Note that the plotted absorbed fraction includes the Compton-thick sources.

Finally, we stress that the model predicts a density of very luminous objects with $L_X \geq 10^{45}$ erg s^{-1} at $z \gtrsim 5$, similar to that at $z \approx 1$. These are the X-ray counterparts of the luminous $M_B \lesssim -27.2$ optical QSOs observed up to $z \approx 6.5$ (see Fan et al. 2004; Richards et al. 2006). This implies that early building up of massive BHs at early epochs is possible in hierarchical scenarios (as long as a constant mass-energy conversion factor $\eta \approx 0.1$ holds; see discussion in the final section). In turn, this is a consequence of the speed up of structure growth (enhanced merging rate) for halos collapsed in biased, high-density regions of the primordial density field, which constitutes a natural feature of hierarchical scenarios.

We now investigate the predictions of our model concerning the luminosity and the redshift dependence of the absorption due to galactic gas. In Figure 3, we show the predicted distributions of the column densities of the absorbers for low-redshift ($z \leq 1$) AGNs with different luminosities, and compare them with data from La Franca et al. (2005) and with predictions based on AGN synthesis models for the cosmic X-ray background (Gilli et al. 2007). The rapid expansion of the blast wave produced by bright AGNs yields a low fraction of absorbed ($N_H \geq 10^{23}$ cm^{-2}), bright ($L_X \geq 10^{45.5}$ erg s^{-1}) AGNs, while at lower luminosity the N_H distribution shifts to larger values. Note that the above relation between the luminosity and the obscuring column density holds

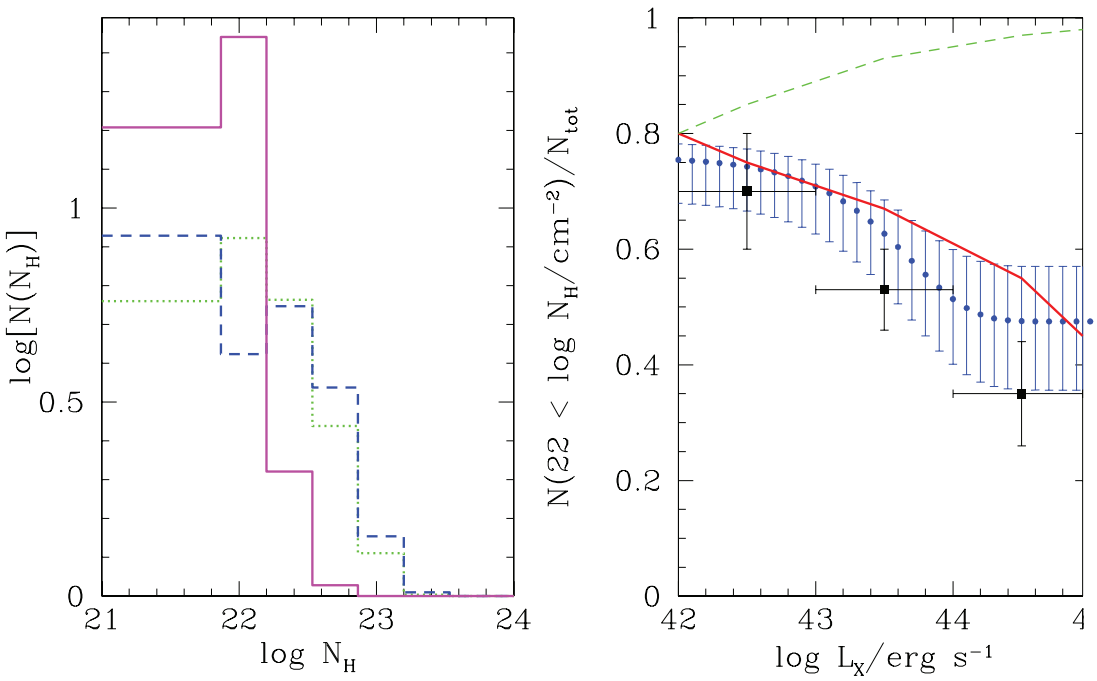

FIG. 3.—*Left*: Distribution of column densities N_H at $z \leq 1$ for AGNs with different luminosities: $42 \leq \log L_X/\mathrm{erg\ s^{-1}} \leq 43$ (*dotted green line*), $43 \leq \log L_X/\mathrm{erg\ s^{-1}} \leq 44$ (*dashed blue line*), and $\log L_X/\mathrm{erg\ s^{-1}} \geq 44$ (*solid violet line*). The lowest N_H bin actually includes the contribution from all absorbing column densities $N_H \leq 10^{22}$ cm^{-2}. *Right*: Predicted fraction of absorbed AGNs with $N_H > 10^{22}$ cm^{-2} as a function of their X-ray luminosities for $z < 1$ (*solid red line*) and compared with data from La Franca et al. (2005) (*filled squares*); the latter have been corrected for the selection effects as described by the authors. We also plot the predictions of the AGN synthesis model for the cosmic X-ray background by Gilli et al. (2007) (*filled blue dots*). We also show the obscured fraction as a function of AGN luminosity when no AGN feedback is considered (*dashed green line*). Note that this has been computed with the same choice of disk parameters, and therefore it is normalized so as to yield the same fraction of obscured AGNs at low luminosities, where the feedback is not effective.

only after averaging over *time after the start of the AGN active phase* and over the *orientations of the galactic disk*, the two fundamental parameters that define the absorption properties of any single AGN in our model. The probability for a line of sight to intercept a given amount of galactic gas is independent of the AGN luminosity (although models predicting such a dependence have been proposed; see Lamastra et al. 2006), while the probability of observing an AGN at a time when the blast wave has depleted the gas content of the galaxy is larger for luminous AGNs, since these produce faster blast waves.

We stress that the inverse correlation between the fraction of obscured objects and luminosity constitutes a key test for AGN feedback as a source of the luminosity dependence of AGN obscuration; indeed, when such feedback is not included, an opposite correlation is found (as shown in Fig. 3), since more luminous AGNs result when a larger fraction of cold gas is available for both accretion and obscuration. Note that qualitatively similar results are obtained for a range of AGN feedback efficiency $2 \times 10^{-2} \leq \epsilon_{\mathrm{AGN}} \leq 2 \times 10^{-1}$. Values outside this range would principally violate constraints set by galaxy colors, the $M_{\mathrm{BH}} - \sigma$ correlation, and the specific star formation rate of massive galaxies at high redshifts.

The overall absorption is expected to evolve strongly with redshift, as shown in Figure 4, where we plot as a function of z the fraction of AGNs (with any luminosity) absorbed by gas with column density $N_H \geq 10^{23}$ cm^{-2}. Such a fraction of absorbed AGNs rises appreciably with redshift, in agreement with the observational findings by La Franca et al. (2005). Although there is still some disagreement among observers on whether the AGN obscuration is dependent purely on luminosity or on both luminosity and redshift (see Gilli et al. 2007 and references therein), the latter case constitutes a generic expectation of models in which obscuration is generated on host galaxy scales. This is due to the larger fraction of cool galactic gas available for both BH accretion and AGN absorption at high redshifts. In turn, this is due to the rapid gas cooling corresponding to the higher densities of the collapsed structures hosting the AGNs, and to the frequent galaxy merging events which continuously replenish the cold gas turned into stars at high redshift. Note that in our model, the fraction of obscured objects with $N_H \geq 10^{22}$ cm^{-2} plotted in Figure 4 includes Compton-thick sources, since it does not resolve the inner regions of AGNs. These are the regions where the Compton-thick absorbers are presumably located, according to several observational indications, from the local abundance of Compton-thick sources (favoring large covering factors and consequently compact sizes; Risaliti et al. 1999), to the direct limits from *Chandra* observations of the Circinus galaxy (see Guainazzi et al. 2001 and references therein), to the rapid oscillation timescale of the absorber in NGC1365 (Risaliti et al. 2005b). In the figure, we tentatively estimate the size of the contribution of Compton-thin sources (*dotted black line*) to the obscured fraction by assuming that the difference between the predicted and the observed densities of AGNs shown in Figure 2 is entirely due to Compton-thick sources. Finally, in Figure 4 we give our predictions for the redshift evolution of the absorbed fraction of AGNs with different luminosities, which are shown by the thinner lines in Figure 4. Note that for $z \gtrsim 2$, the luminosity dependence of the absorbed fractions weakens for AGNs with $L_X \lesssim 3 \times 10^{44}$ erg s^{-1}, while it exhibits a sharp transition to low values $\lesssim 0.5$ for brighter AGNs.

Such a combined luminosity and redshift dependence of AGN absorption, which constitutes a specific prediction of our model, is shown in Figure 5 for a continuous, wide range of luminosities and redshifts. As redshift increases, the overall fraction of absorbed AGNs increases, but with a luminosity dependence much weaker than that at low z (represented in Fig. 2) for luminosities $L_X \lesssim 3 \times 10^{44}$ erg s^{-1}. In fact, the quantity of absorbing gas is

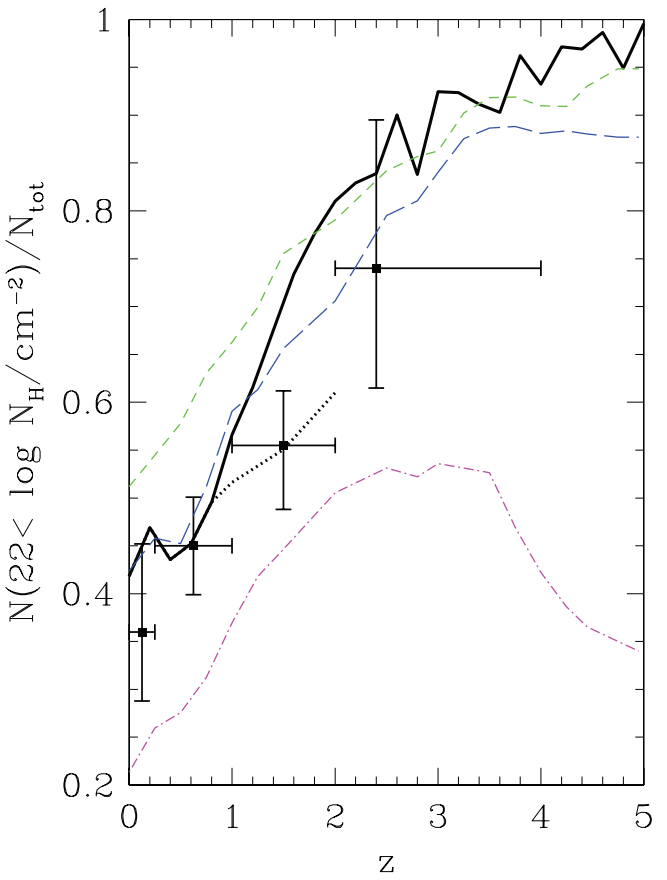

FIG. 4.—Evolution of the predicted fraction of absorbed ($N_H \geq 10^{22}$ cm^{-2}) AGNs for all sources with $43 \leq \log L_X/\mathrm{erg\ s^{-1}} \leq 46$ (*heavy solid black line*). The data from La Franca et al. (2005) have been corrected for the selection effects. The heavy dotted black line represents the contribution to the fraction of absorbed AGNs due to only Compton-thin sources estimated assuming that the difference between the observed and the predicted AGN density in Fig. 2 is entirely due to the Compton-thick AGNs. The thin lines correspond to the absorbed fraction of AGNs within luminosity bins of width 0.25 dex centered on the following values: $L_X/\mathrm{erg\ s^{-1}} = 43.25$ (*green short-dashed line*), $L_X/\mathrm{erg\ s^{-1}} = 44.25$ (*blue long-dashed line*), and $L_X/\mathrm{erg\ s^{-1}} = 44.7$ (*violet dot-dashed line*).

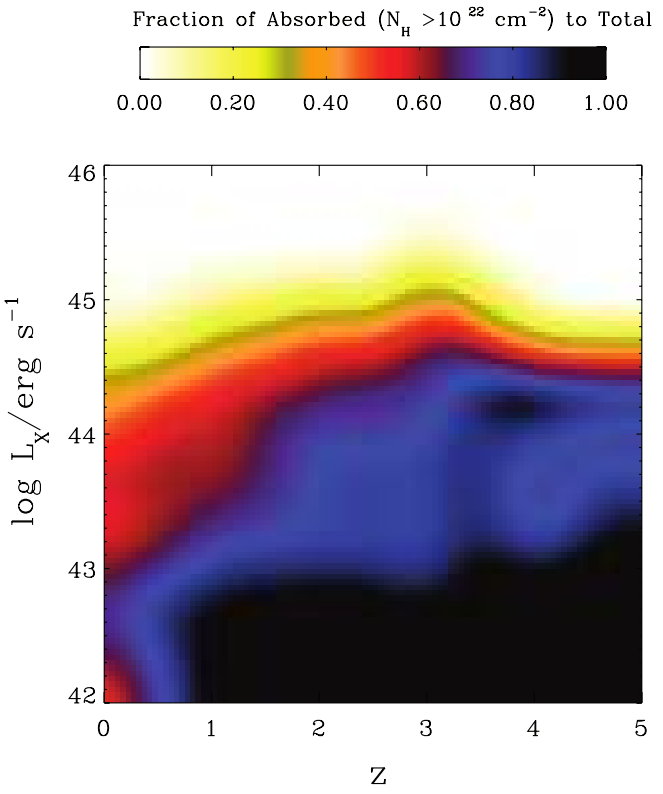

FIG. 5.—Combined luminosity and redshift dependence of the absorbed fraction of AGNs, according to the color code shown on top.

predicted to be large enough (due to the processes discussed above) to make the expanding blast wave induced by the AGN feedback ineffective in expelling a major fraction of the galactic gas, which is continuously replenished in the galactic potential wells. For higher luminosities at $z \gtrsim 2$, a sharp transition occurs between a highly obscured population with $L_X \lesssim 3 \times 10^{44}$ erg s^{-1} and an almost unobscured population with $L_X \gtrsim 10^{45}$ erg s^{-1}. Thus, a testable prediction of our model is that for intermediate luminosities ($10^{43} \lesssim L_X/\mathrm{erg\ s^{-1}} \lesssim 10^{45}$), the ratio of optical to X-ray luminosity functions at redshifts $z \gtrsim 2$ should be much lower than that at $z = 0$, while for higher luminosities it remains close to the local value.

5. SUMMARY AND CONCLUSIONS

We have computed the effects of galactic absorption on AGN emission in a cosmological context by including a physical model for AGN fueling and feedback into a semianalytic model of galaxy formation in concordance cosmology. The model is based on galaxy interactions as triggers for AGN accretion and on expanding blast waves as a mechanism to propagate outwards the AGN energy injected into the interstellar medium at the centers of galaxies.

We have shown that an inverse dependence of AGN absorption on luminosity (Fig. 3) and a direct dependence on redshift (Fig. 4) is a natural result in such a context. The former arises from the faster expansion of blast waves induced by the feedback of energetic, luminous AGNs onto the galactic interstellar gas. The rapid sweeping of gas in the inner regions, where the density is initially higher, results in the fast formation of a gas-depleted region whose size increases for higher AGN intrinsic luminosities. Qualitatively similar conclusions were reached by Hopkins et al. (2005b) on the basis of dedicated hydrodynamical *N*-body simulations. On the other hand, the redshift dependence of the AGN absorption is due to the larger amount of cold galactic gas available at high redshift, when higher densities allow for the fast cooling occurring in galactic halos. The quantitative predictions of our model are consistent with existing observations concerning the fraction of absorbed ($N_H \geq 10^{22}$ cm^{-2}) AGNs as a function of their luminosity and redshift. Our model specifically predicts that for AGNs with $L_X \leq 3 \times 10^{44}$ erg s^{-1}, the luminosity dependence of the absorbed fraction weakens with increasing redshift (see Fig. 5), while for the brightest objects with $L_X \gtrsim 3 \times 10^{44}$ erg s^{-1}, the absorbed fraction quickly decreases with luminosity for $z \gtrsim 2.5$ (see Fig. 5).

Note that, after averaging over the line of sight, unobscured or mildly obscured AGNs correspond to late stages of feedback action; in particular, for a given orientation of the line of sight, the observed column density depends on the time elapsed since the start of the blast wave expansion. The faster expansion characterizing the blast wave of luminous AGNs thus corresponds to a larger probability that we will observe them when the blast has already swept out the central regions of the galaxy's intergalactic medium. This picture constitutes an *extension* of the unified picture for AGNs (see Antonucci 1993) beyond the canonical scheme based on the single orientation parameter, since the absorption properties now depend on the combination of orientation and time needed to sweep the central regions of the

galaxy disk. Note that our picture also has straightforward implications for the connection between star formation and obscuration properties, since from our results we expect, on average, to find larger star formation in heavily obscured objects, while luminous, mildly absorbed AGNs should generally be associated with galaxies with lesser star formation (or that are even in transition to a passive state). The relevance of evolutionary effects of the kind modeled here in determining the absorption properties of AGNs is supported by several observational works. Stevens et al. (2005) and Page et al. (2004) find that X-ray–obscured QSOs have much higher submillimeter detection rates than X-ray–unobscured QSOs, suggesting strong star formation ongoing in the host of obscured AGNs only. Sajina et al. (2007) and Martinez-Sansigre et al. (2008) report *Spitzer* IRS spectra dominated by the AGN continuum but showing features of polycyclic aromatic hydrocarbons (PAHs) in emission, typical of star-forming galaxies, in samples of ultraluminous infrared galaxies (ULIRGs) and radio-selected obscured QSOs at $z \sim 2$. Lacy et al. (2007) find evidence for dust-obscured star formation in type 2 QSOs. Finally, Martinez-Sansigre et al. (2005, 2008) found little or no Lyα emission in a sample of $z > 1.7$ obscured QSOs, suggesting large-scale (kpc) dust distribution. All these findings are in general agreement with the evolutionary picture, although some dissenting works argue for a predominance of geometrical effects (see Triester et al. 2008). A geometrical effect may be constituted by the gravitational bending of the interstellar gas due to the BH, as described in Lamastra et al. (2006); however, except for very massive BHs ($M_{\rm BH} \sim 10^9\ M_\odot$), this will mainly affect regions below our resolution scale of 50 pc. Another class of geometrical models, based on the luminosity dependence of the sublimation radius of the BH accretion disk, is commonly referred to as the "receding torus" picture (Lawrence 1991). These, however, show an appreciable luminosity dependence only at very high AGN luminosities $L_{\rm X} \gtrsim 10^{44}$–$10^{45}$ erg s^{-1} and for dust located close to the sublimation radius (1–10 pc). Dust located in the galaxy disk can hardly be affected directly by the AGN radiation.

In our model, we did not try to model the processes leading to Compton-thick absorption with $N_{\rm H} \geq 10^{24}$ cm^{-2}, generally thought to be caused by gas directly associated with the central regions of AGNs. However, our model provides a hint about the expected luminosity and redshift dependence of the abundance of Compton-thick sources. Inspection of Figure 2, where we compare the predicted global (including Compton-thick sources) density of AGNs with different *intrinsic* luminosities with data corrected for absorption (but not including Compton-thick sources), shows that our model predicts a number of low-/intermediate-luminosity AGNs ($L_{\rm X} \leq 10^{44}$ erg s^{-1}) larger than the observed Compton-thin sources by a factor of $\approx$2 at $z \gtrsim 2$. While it is possible that our model overestimates the AGN fueling in this range of $L_{\rm X}$ and z (e.g., due to its specific modeling of interaction-driven destabilization of cold gas in galactic disks), the above excess could support the view that at such luminosities and redshifts, approximately 1/2 of the total AGNs are Compton thick. A complementary process which could explain our overprediction of low-luminosity AGNs at $z \gtrsim 2$ is suppression of BH growth in small-mass galactic halos (DM masses $M \leq 10^9\ M_\odot$). This could be provided by a gravitational rocket effect on the BHs due to the recoil following the emission of gravitational waves during the coalescence of BH binaries following galaxy mergers (see Madau & Quataert 2004). Such a recoil may produce BH velocities on the order of 10^2 km s^{-1}, which is sufficient to unbind the hole from galaxies with DM velocity dispersions $\lesssim$50 km s^{-1}. In this respect, the observational selection of Compton-thick sources by combining midinfrared to near-infrared and optical photometry of galaxies (Fiore et al. 2008a, 2008b) will provide crucial constraints on the relative role of obscuration and BH depletion in low-mass galactic halos.

Our results are also relevant for constraining the physical mechanisms of AGN feedback onto the interstellar gas, an extremely important issue in the recent developments of cosmological galaxy formation models. Indeed, the recent realizations of such models include AGN feedback as the key process that suppresses gas cooling in massive galactic halos. Actually, two kinds of feedback are at present implemented in this context. On the one hand, models based on galaxy interactions as triggers of AGN activity and feedback envisage the latter to be associated with the bright accretion phase onto supermassive black holes, i.e., to the same phase as that corresponding to AGN activity (see Menci et al. 2003, 2006; Di Matteo et al. 2005; Hopkins et al. 2005a). On the other hand, other authors associate the AGN feedback with a quiescent (so-called "radio") phase of accretion, characterized by extremely low accretion rates ($\lesssim 10^{-2}\ M_\odot$ yr^{-1}) and, hence, not observable as radiative AGNs (Bower et al. 2006; Croton et al. 2006). Since the latter case would result in feedback activity that continues down to low redshift, we expect such models to show a much milder dependence of AGN absorption on redshift, so that observational results on the high-redshift absorption of AGN emission will constitute an effective test for models of AGN feedback.

Finally, we note that the feedback related to the active AGN phase described here is effective in decreasing the galactic gas and the associated absorption mainly at low redshift $z \lesssim 2$ and for bright ($L_{\rm X} \gtrsim 10^{44}$ erg s^{-1}) AGNs (see, e.g., Cavaliere & Menci 2007). This implies that at high redshifts, the effective cooling and the continuous replenishing of galactic gas due to frequent merging events will override the depletion due to AGN feedback, so the latter will not suppress the early growth of supermassive BHs. Indeed, the predicted number density of early ($z \geq 4$), bright ($L_{\rm X} \geq 10^{45.5}$ erg s^{-1}) AGNs shown in Figure 2 is consistent with that observed for bright ($M_i \leq -27.5$) optical QSOs up to $z \approx 6$ (Hopkins et al. 2006). Note, however, that such a result does not include the BH spin up that may occur during the growth due to gas accretion (for a different modeling of such a process, see, e.g., Volonteri et al. 2005; King et al. 2008), which in turn may yield larger radiation efficiencies up to values $\eta \approx 0.3$ for a dominant fraction of BHs. As noted by the above authors, the lower mass accretion rate caused by larger radiation efficiencies may delay the mass assembly of massive BHs at early epochs when included in a cosmological model. We shall investigate these issues in a following paper.

We thank the referee for helpful comments which helped to improve the paper. We acknowledge grants from ASI.

APPENDIX A

APPENDIX

The key quantity determining the blast wave evolution is the energy deposition ratio $\Delta E/E$ between the energy injected up to time t and the ISM energy out to the shock radius at the same time. This is constant in self-similar solutions, which imply for the energy injection the

law $\Delta E(t) \propto t^{2(5-2\omega)/\omega}$ (§ 5 and Appendix C2 of Lapi et al. 2005), normalized to yield the total value $\Delta E = \eta \epsilon_{\rm AGN} \Delta m_{\rm acc}$ (eq. [4]) at the end of the AGN active phase. Its time behavior is thus related to the exponent ω, which defines the decline of the gas density distribution.

Since the supersonic wave affects the plasma only out to the shock distance $R_s(t)$, where the unperturbed (initial) energy content is $E(<R_s(t)) \propto R_s(t)^{5-2\omega} \propto t^{2(5-2\omega)/\omega}$ (Lapi et al. 2005), the ratio $\Delta E/E$ is constant, and it constitutes the basic quantity determining the strength of the shock; in other words, $\Delta E/E$ remains constant while the wave expands, since both the energy injected up to the considered time and the ISM energy content within the shock radius increase with time according to the same law. Thus, we choose to compute $\Delta E/E$ as the total energy injected by the AGN divided into the total energy content of the ISM (within the whole volume of the disk).

The luminosity L is the time derivative of ΔE, and thus in the self-similar model it is to behave as $L = d\Delta E/dt \propto t^{5(2-\omega)/\omega}$, so its decay is related to the exponent ω, which defines the density decline (see Lapi et al. 2005, § 5 and Appendix C2).

For our piecewise approximation of the density profile (point [2] in § 3.2), L is constant during the time when the wave sweeps the inner region $r \leq r_d/2$, declines as $L \propto t^{-0.65}$ when the blast has expanded into the region $r_d/2 < r \leq 3r_d/2$, and then drops to zero when $r > 3r_d/2$, where ΔE remains constant at the value attained at the border $r = 3r_d/2$, which is consistent with the index $\omega = 5/2$ holding in that region.

Full consistency with the self-similar blast wave model would require us to assign each AGN a time-dependent luminosity, decaying as described above. However, the results are indistinguishable from those obtained with the simple prescription $L =$ constant (provided both luminosities are normalized to the same final total injection ΔE) for two reasons.

1. In the central $r \leq r_d/2$ region, L is indeed constant, as we have shown above; in the outer region, the self-similar behavior $L \propto t^{-0.65}$ results in a decay of the luminosity much slower than the decline of the ISM density encountered by the blast $\rho \propto R_s^{-\omega}$. In fact, using equation (5) for the time expansion of $R_s(t) \propto t^{2/\omega}$, the density in front of the blast declines as $\rho \propto t^{-2}$. Clearly, the regime when the blast expands into the outer region $r = 3r_d/2$ is not important, since here the luminosity is null, and the object is not recognized as an active AGN in computing the $N_{\rm H}$ distributions shown in § 4.
2. Most important, the scale height of the disk $h = r_d/15$ is much shorter than the radius $r_d/2$ enclosing the first radial shell that we use to fit the exponential profile of the disk. This in turn means that nearly all the random lines of sight that we draw from the galaxy center only intercept the first radial shell, where the luminosity is effectively constant according to the self-similar construction of the model. Quantitatively, the probability for a line of sight to intercept the outer ($r > r_d/2$) disk is $[\arctan(2/15)]/(\pi/2) \approx 8 \times 10^{-2}$. Beyond the details of our specific self-similar blast wave model, the physical point is that the geometry of the disk is such that the vast majority of the lines of sight are only affected by the inner region; this is completely swept by the blast early on, when the luminosity decay has not yet occurred.

REFERENCES

Antonucci, R. 1993, ARA&A, 31, 473
Ballantyne, D. R., Everett, J. E., & Murray, N. 2006, ApJ, 639, 740
Barcons, X., Mateos, S., & Ceballos, M. T. 2000, MNRAS, 316, L13
Begelman, M. C. 2003, in Coevolution of Black Holes and Galaxies, ed. L. C. Ho (Cambridge: Cambrdidge Univ. Press), 374
Bond, J. R., Cole, S., Efstathiou, G., & Kaiser, N. 1991, ApJ, 379, 440
Bower, R. G., et al. 2006, MNRAS, 370, 645
Cavaliere, A., Lapi, A., & Menci, N. 2002, ApJ, 581, L1
Cavaliere, A., & Menci, N. 2007, ApJ, 664, 47
Cavaliere, A., & Vittorini, V. 2000, ApJ, 543, 599
Chartas, G., Brandt, W. N., Gallagher, S. C., & Garmire, G. P. 2002, ApJ, 579, 169
Churazov, E., Brüggen, M., Kaiser, C., Bringer, H., & Forman, W. 2001, ApJ, 554, 261
Crenshaw, D. M., Kraemer, S. B., & George, I. M. 2003, ARA&A, 41, 117
Croton, D. J., et al. 2006, MNRAS, 365, 11
Di Matteo, T., Springel, V., & Hernquist, L. 2005, Nature, 433, 604
Elvis, M. 2000, ApJ, 545, 63
———. 2006, Mem. Soc. Astron. Italiana, 77, 573
Fan, X., et al. 2004, AJ, 128, 515
Ferrarese, L., & Merritt, D. 2000, ApJ, 539, L9
Fiore, F., et al. 2008a, ApJ, 672, 94
———. 2008b, ApJ, submitted
Fontanot, F., Monaco, P., Christiani, S., & Tozzi, P. 2006, MNRAS, 373, 1173
Gallimore, J. F., Baum, S. A., & O'Dea, C. P. 1997, Nature, 388, 852
Gebhardt, K., et al. 2000, ApJ, 539, L13
Gilli, R., Comastri, A., & Hasinger, G. 2007, A&A, 463, 79
Granato, G. L., De Zotti, G., Silva, L., Bressan, A., & Danese, L. 2004, ApJ, 600, 580
Guainazzi, M., Fiore, F., Matt, G., & Perola, G. C. 2001, MNRAS, 327, 323
Hasinger, G. 2008, A&A, submitted (arXiv:0808.0260)
Hopkins, P. F., Hernquist, L., Cox, T. J., Di Matteo, T., Martini, P., Robertson, B., & Springel, V. 2005a, ApJ, 630, 705
Hopkins, P. F., Hernquist, L., Cox, T. J., Di Matteo, T., Robertson, B., & Springel, V. 2005b, ApJ, 632, 81
———. 2006, ApJS, 163, 1
King, A. R., Pringle, J. E., & Hofmann, J. A. 2008, MNRAS, 385, 1621
Lacey, C. G., & Cole, S. 1993, MNRAS, 262, 627
Lacy, M., et al. 2007, ApJ, 669, L61
La Franca, F., et al. 2005, ApJ, 635, 864
Lamastra, A., Perola, G. C., & Matt, G. 2006, A&A, 449, 551
Lapi, A., Cavaliere, A., & Menci, N. 2005, ApJ, 619, 60
Lawrence, A. 1991, MNRAS, 252, 586
Lawrence, A., & Elvis, M. 1982, ApJ, 256, 410
Madau, P., & Quataert, E. 2004, ApJ, 606, L17
Madau, P., & Rees, M. J. 2001, ApJ, 551, L27
Malkan, M. A., Gorjian, V., & Tam, R. 1998, ApJS, 117, 25
Marconi, A., Risaliti, G., Gilli, R., Hunt, L. K., Maiolino, R., & Salvati, M. 2004, MNRAS, 351, 169
Martinez-Sansigre, A. Lacy, M., Sajina, A., & Rawlings, S. 2008, ApJ, 674, 676
Martinez-Sansigre, A., et al. 2005, Nature, 436, 666
———. 2007, MNRAS, 379, L6
Matt, G. 2000, A&A, 355, L31
McNamara, B. R., & Nulsen, P. E. J. 2007, ARA&A, 45, 117
Menci, N., Cavaliere, A., Fontana, A., Giallongo, E., & Poli, F. 2004, ApJ, 604, 12
Menci, N., Cavaliere, A., Fontana, A., Giallongo, E., Poli, F., & Vittorini, V. 2003, ApJ, 587, L63
Menci, N., Fontana, A., Giallongo, E., Grazian, A., & Salimbeni, S. 2006, ApJ, 647, 753
Menci, N., Fontana, A., Giallongo, E., & Salimbeni, S. 2005, ApJ, 632, 49
Morganti, R., Tadhunter, C. N., & Oosterloo, T. A. 2005, A&A, 444, L9
Murray, N., Quataert, E., & Thompson, T. A. 2005, ApJ, 618, 569
Nagar, N. M., & Wilson, A. S. 1999, ApJ, 516, 97
Narayan, C. A., & Jog, C. J. 2002, A&A, 394, 89
Nulsen, P. E. J., & Fabian, A. C. 2000, MNRAS, 311, 346
Page, M. J., Stevens, J. A., Ivison, R. J., & Carrera, F. J. 2004, ApJ, 611, L85
Pounds, K., King, A. R., Page, K. L., & O'Brien, P. T. 2003, MNRAS, 346, 1025
Pounds, K., & Page, K. L. 2006, MNRAS, 372, 1275
Pozzi, F., et al. 2007, A&A, 468, 603
Proga, D. 2007, ApJ, 661, 693
Reynolds, C. S., Heinz, S., & Begelman, M. C. 2001, ApJ, 549, L179
Richards, G. T., et al. 2006, AJ, 131, 2766
Richstone, D., et al. 1998, Nature, 395, A14
Risaliti, G., Bianchi, S., Matt, G., Baldi, A., Elvis, M., Fabbiano, G., & Zezas, A. 2005a, ApJ, 630, L129
Risaliti, G., Elvis, M., Fabbiano, G., Baldi, A., & Zezas, A. 2005b, ApJ, 623, L93
Risaliti, G., Maiolino, R., & Salvati, M. 1999, ApJ, 522, 157

Sajina, A., et al. 2007, ApJ, 664, 713
Salim, S., et al. 2007, ApJS, 173, 267
Saslaw, W. C. 1985, Gravitational Physics of Stellar and Galactic Systems (Cambridge: Cambridge Univ. Press)
Sedov, L. I. 1959, Similarity and Dimensional Methods in Mechanics (New York: Academic Press)
Spergel, D. N., et al. 2007, ApJS, 170, 377
Stevens, J. A., et al. 2005, MNRAS, 360, 610
Thean, A. H. C., Gillibrand, T. I., Pedlar, A., & Kukula, M. J. 2001, MNRAS, 325, 737
Triester, E., Krolik, J. H., & Dullemond, C. 2008, ApJ, 679, 140
Turnshek, D. A., Grillmair, C. J., Foltz, C. B., & Weymann, R. J. 1988, ApJ, 325, 651
Ueda, Y., Akiyama, M., Ohta, K., & Miyaji, T. 2003, ApJ, 598, 886
Volonteri, M., Madau, P., Quataert, E., & Rees, M. J. 2005, ApJ, 620, 69
Weymann, R. J. 1981, ARA&A, 19, 41
Yu, Q., & Tremaine, S. 2002, MNRAS, 335, 965